42. Matthias E, in *Hyperfine Structure and Nuclear Radiation*: *Proc. of a Conf., USA, August 25–30, 1967* (Eds E Matthias, D A Shirley) (Amsterdam: North-Holland, 1968) p. 815
43. Pfeiffer L, Heiman N D, Walker J C *Phys. Rev. B* **6** 74 (1972)
44. Mitin A V *Zh. Eksp. Teor. Fiz.* **52** 1596 (1967) [*Sov. Phys. JETP* **25** 1062 (1967)]
45. Heiman N D, Walker J C, Pfeiffer L *Phys. Rev.* **184** 281 (1969)
46. Yakimov S S et al. *Pis'ma Zh. Eksp. Teor. Fiz.* **26** 16 (1977) [*JETP Lett.* **26** 13 (1977)]
47. Vagizov F G, Manapov R A, Mitin A V *Opt. Spektrosk.* **51** 941 (1981) [*Opt. Spectrosc.* **51** 522 (1981)]
48. Leksin V V, Manapov R A, Mitin A V *Izv. Akad. Nauk SSSR, Ser. Fiz.* **50** 2362 (1986)
49. Vagizov F G *Hyperfine Interact.* **61** 1359 (1990)
50. Vagizov F G *Hyperfine Interact.* **95** 85 (1995)
51. Tittonen I et al. *Phys. Rev. Lett.* **69** 2815 (1992)
52. Lippmaa M et al. *Phys. Rev. B* **52** 10268 (1995)
53. Mitin A V, in *Nekotorye Voprosy Magnitnoi Radiospektroskopii i Kvantovoi Akustiki*: *Materialy Nauchnoi Konf., Mai 1967, Kazan'* (Some Aspects of Magnetic Radio-Frequency Spectroscopy and Quantum Acoustics. Proc. of a Scientific Conf., May, 1967, Kazan) (Eds B M Kozyrev, U H Kopvillem) (Kazan: KFTI AN SSSR, 1968) p. 120
54. Mitin A V, Chugunova G P *Fiz. Tverd. Tela* **16** 614 (1974) [*Sov. Phys. Solid State* **16** 403 (1974)]
55. Chugunova G P, Mitin A V *Phys. Lett. A* **47** 243 (1974)
56. Mitin A V, Chugunova G P *Phys. Status Solidi A* **28** 39 (1975)
57. Bersuker I B, Borshch S A, Ogurtsov I Ya *Fiz. Tverd. Tela* **15** 2270 (1973) [*Sov. Phys. Solid State* **15** 1518 (1974)]
58. Mitin A V, Polyakov N V *Phys. Status Solidi B* **115** 477 (1983)
59. Mitin A V, in *Proc. of the 5th Intern. Conf. on Mössbauer Spectroscopy, Bratislava, 3–7 September, 1973* (Praha: Czechoslovakia Atomic Energy Commission. Nuclear Information Centre, 1975) p. 615
60. Mitin A V *Phys. Lett. A* **84** 278 (1981)
61. Mitin A V *Izv. Ross. Akad. Nauk, Ser. Fiz.* **56** (7) 186 (1992) [*Bull. Russ. Acad. Sci., Ser. Phys.* **56** 1108 (1992)]
62. Mitin A V, Makarov E F, Polyakov N V *Zh. Eksp. Teor. Fiz.* **90** 1931 (1986) [*Sov. Phys. JETP* **63** 1130 (1986)]
63. Mitin A V, Polyakov N V *Phys. Lett. A* **114** 27 (1986)
64. Voitovetskii V K et al. *Pis'ma Zh. Eksp. Teor. Fiz.* **36** 322 (1982) [*JETP Lett.* **36** 393 (1982)]
65. Mitin A V, Lyubimov V Yu, Sadykov E K *Pis'ma Zh. Eksp. Teor. Fiz.* **81** 538 (2005) [*JETP Lett.* **81** 424 (2005)]
66. Bashkirov Sh Sh, Sadykov E K *Fiz. Tverd. Tela* **20** 3444 (1978) [*Sov. Phys. Solid State* **20** 1988 (1978)]
67. Bashkirov Sh Sh, Belyanin A L, Sadykov E K *Phys. Status Solidi B* **93** 437 (1979)
68. Dzyublik A Ya *Phys. Status Solidi B* **104** 81 (1981)
69. Afanas'ev A M, Aleksandrov P Ya, Yakimov S S, Preprint IAE-3337/9 (Moscow: I V Kurchatov Institute of Atomic Energy, 1980)
70. Mitin A V *Phys. Lett. A* **84** 283 (1981)
71. Mitin A V *Opt. Spektrosk.* **53** 288 (1982) [*Opt. Spectrosc.* **53** 168 (1982)]
72. Mitin A V, Doctoral Thesis of Physico-Mathematical Sciences (Kazan: Kazan Physical-Technical Institute of the USSR Academy of Sciences, 1984)
73. Aleksandrov E B *Usp. Fiz. Nauk* **107** 595 (1972) [*Sov. Phys. Usp.* **15** 436 (1973)]
74. Mitin A V, in *Tezisy Vsesoyuz. Soveshchaniya po Yaderno-Spektroskopicheskim Issledovaniyam Sverkhtonkikh Vzaimodeistvii, Moskva, 1985* (Digest of All-Union Conf. on Nuclear Spectroscopy Studies of Hyperfine Interactions, Moscow, 1985) (Moscow, 1985) p. 110
75. Sadykov E K, Zakirov L L, Yurichuk A A *Laser Phys.* **11** 409 (2001)
76. Sadykov E K et al. *Izv. Ross. Akad. Nauk, Ser. Fiz.* **67** 995 (2003) [*Bull. Russ. Acad. Sci., Ser. Phys.* **67** 1099 (2003)]
77. Harris S E *Phys. Today* **50** (7) 36 (1997)
78. Mitin A V, Roganov D F *Izv. Ross. Akad. Nauk, Ser. Fiz.* **65** 941 (2001) [*Bull. Russ. Acad. Sci., Ser. Phys.* **65** 1020 (2001)]
79. Mitin A V, Aniskin I P, Tarasov V A *Izv. Ross. Akad. Nauk, Ser. Fiz.* **69** 1414 (2005) [*Bull. Russ. Acad. Sci., Ser. Phys.* **69** 1585 (2005)]
80. Dabagov S B *Usp. Fiz. Nauk* **173** 1083 (2003) [*Phys. Usp.* **46** 1053 (2003)]
81. Mitin A V *Phys. Lett. A* **213** 207 (1996)
82. Mitin A V, in *Proc. First Intern. Induced Gamma Emission Workshop 1997, Predeal, Romania* (Eds I I Popescu, C A Ur) (Bucharest: IGE Foundation, 1999) p. 145
83. Mitin A V *Opt. Spektrosk.* **92** 432 (2002) [*Opt. Spectrosc.* **92** 389 (2002)]
84. Mitin A V, Aniskin I P, in *Proc. of 7th AFOSR Workshop on Isomers and Quantum Nucleonics, Dubna, June 26–July 1, 2005*: *Book Abstracts* (Eds S A Kamarin, J J Carroll, E A Cherepanov) (Dubna: JINR, 2006) p. 206
85. Poole C P (Jr.), Farach H A *J. Magn. Res.* **1** 551 (1969)
86. Pfeiffer L *J. Appl. Phys.* **42** 1725 (1971)
87. Kopcewicz M, Wagner H-G, Gonser U *Solid State Commun.* **48** 531 (1983)
88. Shvyd'ko Yu V et al. *Phys. Rev. B* **52** R711 (1995)
89. Shvyd'ko Yu V et al. *Phys. Rev. Lett.* **77** 3232 (1996)
90. Cherepanov V M et al., in *Proc. of the First Intern. Induced Gamma Emission Workshop, Predeal, Romania* (Eds I I Popescu, C A Ur) (Bucharest: IGE Foundation, 1999) p. 394
91. Bersuker I B, Kovarskii V A *Pis'ma Zh. Eksp. Teor. Fiz.* **2** 286 (1965) [*JETP Lett.* **2** 182 (1965)]
92. Bashkirov Sh Sh, Sadykov E K *Pis'ma Zh. Eksp. Teor. Fiz.* **3** 240 (1966) [*JETP Lett.* **3** 154 (1966)]
93. Mitin A V *Fiz. Tverd. Tela* **10** 3632 (1968) [*Sov. Phys. Solid State* **10** 2880 (1969)]
94. Ivanov A S, Kolpakov A V, Kuz'min R N *Fiz. Tverd. Tela* **16** 1229 (1974) [*Sov. Phys. Solid State* **16** 794 (1974)]
95. Letokhov V S *Phys. Rev. A* **12** 1954 (1975)
96. Bashkirov Sh Sh et al. *Pis'ma Zh. Eksp. Teor. Fiz.* **27** 486 (1978) [*JETP Lett.* **27** 457 (1978)]
97. Bibikova Yu F et al. *Fiz. Tverd. Tela* **22** 2349 (1980)
98. Olariu S et al., in *Intern. Conf. of the Applications of the Mössbauer Effect*: *ICAME 2005, Montpellier, France, September 5–9, 2005*, Abstracts, p. T6–P17
99. Vagizov F et al., in *Intern. Conf. of the Applications of the Mössbauer Effect*: *ICAME 2005, Montpellier, France, September 5–9, 2005*, Abstracts, p. T6–P29

PACS numbers: **07.60.–j**, **87.64.–t**

DOI: 10.1070/PU2006v049n09ABEH006096

Methods and tools for the express immunoassay. A new approach to solving the problem

V E Kurochkin

1. Introduction

The rapid development of heterogeneous immunoassay (HetIA) techniques is facilitated by the high specificity of the antigen (Ag)–antibody (At) reaction underlain by the ability of the two molecules to recognize each other in a 'lock and key' fashion. Theoretically, it allows detecting a single molecule (particle) of the study substance in a real-time scale, provided highly sensitive assay methods are available for the purpose along with a mechanism to achieve a rapid transfer of individual Ag to the active centers immobilized at the surface. The practical solution to this problem is paramount for epidemiology, faced with the necessity of identifying causal factors of dangerous infections in multi-component environmental samples.

The proposed concept of the construction of highly sensitive systems for express immunoanalysis is first and

foremost based on the results of research conducted along the following three lines:

1. Purpose-oriented application of physical processes proceeding in the field of an ultrasound standing wave (USSW) for the transport of Ag to the immunosorbent (IS) surface under diffusion and concentration constraints imposed on mass transfer and for the minimization of effects of non-specific sorbing impurities.

2. Development of theoretical propositions of reflection photometry in application to thin-layer optically transparent elements (chemo- and biosensors) for the creation of highly sensitive detectors operating in a real-time regime and optimally fit to the reaction block.

3. Investigation into characteristics of the recurrent stochastic algorithm for processing 'linear trend' signals for the rapid and noise-independent assessment of informative parameters of the signals.

2. Intensification of antigen – antibody reactions using the standing wave of an ultrasonic field

Analysis of different methods for the acceleration of mass-transfer in HetIA has demonstrated that the use of traditional techniques such as a flow regime, intensification of mixing, etc. gives poor results [1 – 3]. The application of ultrasound (US) fields appears more promising, and the author believes that carrying out Ag – At reactions in a noncavitating USSW field of the megahertz range affords significant advantages because it permits

• forming IS layers with a 1/2 US-wavelength periodicity (using the radiation force action on IS particles) [4 – 6];

• retaining suspended IS particles in an US cell in the flow regime by counteracting the Stokes force to be able to change solutions of ingredients [7];

• ensuring noncontact free mixing in microsamples with a given spatial scale L ($L \gg \lambda$ for convective flows, $L \sim \lambda/2$ for Rayleigh flows and $L = (\lambda/4)\, 2\delta$ for Schlichting boundary flows, where $\delta = (\nu/\pi f)^{1/2}$ is the width of the acoustic boundary layer, ν is the kinematic viscosity of the liquid, and f is the oscillation frequency [8]). The boundary layer width under ordinary conditions (water, temperature 20 °C) and $f = 3$ MHz is $\delta \sim 0.3$ μm.

The author of this publication has forwarded a hypothesis that the purpose-oriented creation of the Rayleigh flow or a combination of the Rayleigh and Schlichting flows may lay the basis for a new universal and rapid mechanism of Ag transfer to the IS surface. A flow speed proportional to the average acoustic energy E [8] (hence, controllable in a broad range) should be chosen in order (a) to substantially increase the velocity of mass transfer, i.e., the probability of the meeting of Ag and At; (b) not to interfere with specific interactions (in other words, the kinetic energy of Ag must be smaller than the Ag – At coupling energy); (c) to decrease the probability of nonspecific interactions between sample components and the IS surface; and (d) to ensure rapid and efficient removal of nonspecifically sorbed components of the sample at the wash-out stage.

For Ag of bacterial origin, USSW allows realizing an additional mechanism, that is, Ag transfer to the IS surface under the effect of radiation forces, which results in the concentration of particles at pressure nodes and antinodal points (depending on the medium and particle properties). The efficiency of such a mechanism increases with increasing the size of the particles. (At a certain ratio of densities and compressibilities of the particles and the medium, this mechanism may slow down and even completely block particle transfer by acoustic flows.)

The experimental arrangement used to verify the above hypothesis and the possibility of practical realization of the proposed mechanism are depicted in Fig. 1. It consists of two blocks, one for specific reactions at IS microspheres and the other for fluorescence detection. The former block includes an US-emitter, removable reaction microchambers (15, 20, and 25 μl), pumps for the introduction of reaction ingredients, and a thermostatic liquid. A microchamber is installed in the focus of objective lens *11* (see Fig. 1) that serves to feed a beam of exciting radiation onto reaction products and to collect an informative signal.

The working parameters of the device are $f = 1 - 4$ MHz, $E = 1 - 10$ J m^{-3}, and the pumping speed $u = 0.02 - 0.50$ cm s^{-1}.

The immunosorbent is prepared from optically transparent agarose or sepharose spherical beads of radius $R = 15$ μm.

In preliminary studies, the dependence of particle retention on E, f, u, and R was evaluated and optimal conditions were chosen for the complete retention of IS particles in the flow at the bulk velocity up to 1 ml min^{-1}. Methods were developed for the formation of a desired number of compact IS monolayers ($\geqslant 1$) parallel to the emitter plane in one- and two-wave US-chambers.

The efficiency of the proposed mechanism for the intensification of Ag – At reactions was assessed by comparing analytical characteristics obtained in analyses using the USSW technique and a traditional method [9], i.e., mixing by repeated pipetting on a microplate. The principal analytical

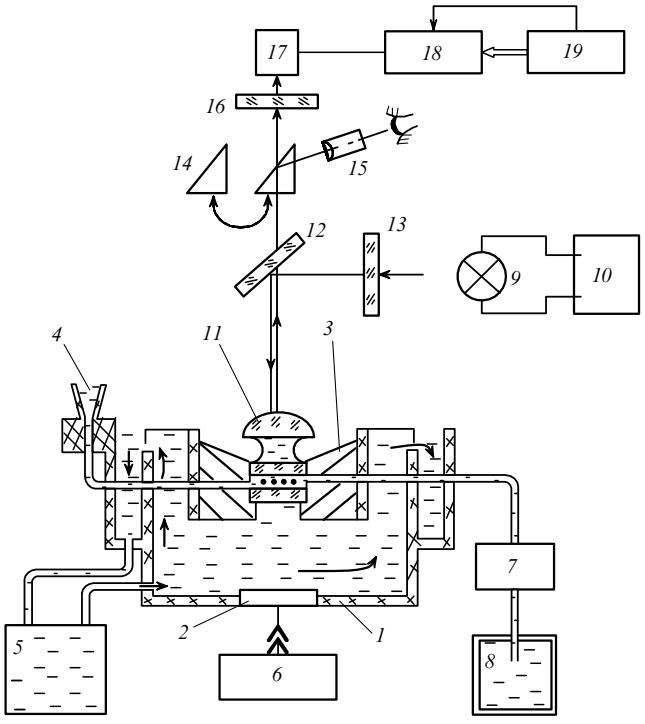

Figure 1. Diagram of experimental set-up: *1* — support of the US-emitter, *2* — US-emitter, *3* — microchamber, *4* — microfunnel, *5* — pump with a thermostat, *6* — high-frequency generator (HFG), *7* — peristaltic pump, *8* — container, *9*, *10* — radiation source, *11* — objective lens, *12*, *13*, *16* — light filters, *14* — rotary prism, *15* — eye-piece, *17* — photoelectronic multiplier (PEM), *18* — analog-digital converter (ADC), *19* — computer.

characteristics include the time necessary for the reaction to be completed (t_p), the duration of the wash-out procedure (t_o), and the sensitivity or detection limit (DL). The antigens being studied differ in size (immunoglobulins, toxins, viruses, and bacteria).

The results of experiments indicate that t_p depends on antigen dimensions (Fig. 2a), but even in the 'worst case' (large Brucella bacteria), the use of a US-field allows t_p to be reduced 25-fold (to less than 90 s) compared with the reaction time in the traditional method (curve *3* in Fig. 2a and the curve in Fig. 2b, respectively).

The use of US-fields not only permits diminishing t_p but also makes the wash-out procedure for the removal of non-specifically absorbed impurities three times shorter. This result is achieved by combining the flow regime and the action of acoustic boundary flows (Fig. 2a).

The applicability of the method in question for practical purposes was checked by assaying coded samples that contained the threshold or higher concentrations of heterologous microorganisms and toxins as impurities, as well as dust and some biologically active compounds (at the total concentration 0.125 – 0.25 mg ml^{-1}). The type and amount of admixtures added to the samples were varied according to the law of random numbers. The incubation time was 120 s. Based on the analysis of 65 samples, the assay sensitivity was 1, the specificity was 0.95, the relative risk tended to 0, and the frequency of false positive and false negative results was 1/45 and 0, respectively.

These results and estimates of the DL (see the Table) indicate that the mechanism of HetAI intensification proposed and realized by the author provides a rapid and reliable tool for the detection of single pathogenic organisms in microsamples containing interfering impurities. (An US cell contained 10 and 2 microbial bodies of brucellosis and tularemia bacteria, respectively).

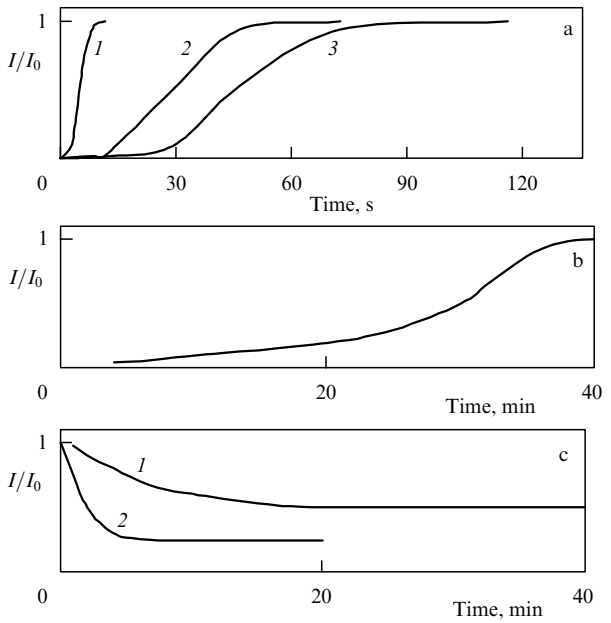

Figure 2. Plots of the luminescence intensity versus the incubation time (a), (b) and wash-out time (c). Figure 2a shows reactions of antigens in an USSW: curve *1* — immunoglobulins ($D \sim 0.04$ μm), curve *2* — chlamydine ($D \sim 0.3$ μm), curve *3* — brucellas (0.4×1.2 μm); Fig. 2b — traditional method (brucella antigen); Fig. 2c: curve *1* — traditional wash-out procedure, curve *2* — washing out in an USSW.

Table. Evaluation of express assay sensitivity.

Immunoactive subject	Sensitivity, microbial bodies per 1 cm^2 (dilution)	
	Instrument	Reference method
Tularemia bacteria	1×10^2	1×10^4
Tetanus toxoid anatoxin	(1 : 1000)	(1 : 200)
Brucellas	5×10^2	1×10^4
Smallpox vaccine virus	(1 : 200)	(1 : 1)
Rickettsia D. *sibiricus*	(1 : 2000)	(1 : 250)

The novelty of the proposed method is protected by the inventor's certificates [10, 11] and the experimental data are published in part in Ref [12].

The validity of the USSW application concept developed by the author and the related technical decisions was confirmed by other researchers who proposed a similar variant of the construction of one- and two-wave chambers for the examination of particle aggregation and acoustic flows in USSW [13], used the Rayleigh acoustic flow and flow US-chambers for the acceleration of mass transfer toward live indicator cells in order to evaluate aquatic toxicity [14], and applied the USSW technique to improve assay sensitivity for the detection of bacterial spores by HetIA in flow chambers [15]. (The last two publications are lacking in the assessment of the applicability of the devices and methods used for the analysis of real samples.)

3. Principles of the construction of highly sensitive optical detectors

Classical photometry of thin-layer objects (IS monolayers in one- or two-wave US cuvettes and optical sensors based on selective plasticized membranes) in transmitted light is associated with impaired sensitivity of the analysis [16]. At the same time, it is known [17] that diffuse radiation is absorbed more effectively than directed radiation, while multiple reflections of the light flux automatically lead to the lengthening of the optical path. It may therefore be expected that mounting thin optically transparent sensitive elements (SEs) on a diffusely reflective substrate and measurements in the transmitted light would substantially improve the assay sensitivity. Adequate theoretical models lacking [18 – 20], we think it appropriate to describe light propagation processes in SEs of a restricted size that are optically conjugated with the reflective substrate.

The sensitive element is a cylinder of diameter D and height l made from an optically transparent material (Fig. 3) and characterized by the dimensionless parameter $g = D/l$, the refraction index n, and the coefficient of extinction ε. The substrate has the reflection coefficient $\rho_b(\Theta')$ and the refraction index n_b.

It is assumed that (a) the light-absorbing components are uniformly spread over the SE volume and the transmission obeys Beer's law, that is, it changes with varying the concentration of the components; (b) the coefficient of light flux reflection near the critical angle Θ_c of the complete inward reflection (CIR) changes jump-wise, and (c) the average height of SE and reflective substrate roughness is much smaller than the probing radiation wavelength.

Let a parallel light flux with the intensity I_0 and transverse cross section $d < D$ be incident perpendicular to the SE surface. (Beams reflected from the substrate are incident on

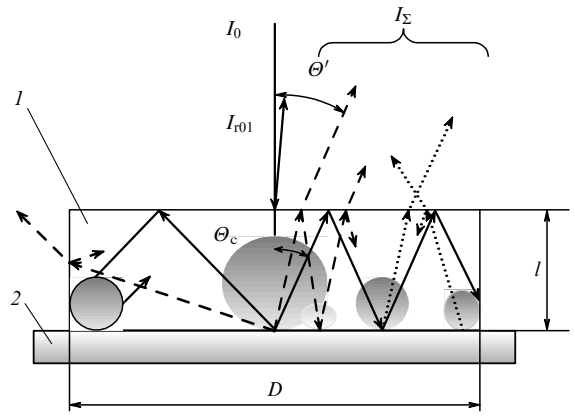

Figure 3. Schematic of light flow distribution in a thin-layer optically transparent element *1* (restricted in size) on a reflecting substrate *2* (see text for details).

the SE – air interface at an angle Θ.) Then, the total intensity of the light flux I_Σ outgoing from SE at an angle Θ' can be written as

$$I_\Sigma = I_0 B(\Theta')[\Phi_1+\Phi_2+\Phi_3+\Phi_4]\,\exp\left[-\varepsilon l\left(1+\frac{1}{\cos\Theta'}\right)\right], \tag{1}$$

where

$$B(\Theta') = \left[1-\rho_{10}(\Theta')\right]\left[1-\rho_{01}\right]\rho_b(\Theta'),$$

$$\Phi_1 = \frac{E(0)\exp(-2\varepsilon l)}{1-E(0)\exp(-2\varepsilon l)},$$

$$\Phi_2 = \int_\delta^{\Theta_1} \frac{\mathrm{d}\Theta}{1-E(\Theta)\exp(-2\varepsilon l/\cos\Theta)},$$

$$\Phi_3 = \rho_c \int_{\Theta_1}^{\Theta_2} \frac{\exp(-2\varepsilon l/\cos\Theta)\,\mathrm{d}\Theta}{1-E(\Theta)\exp(-2\varepsilon l/\cos\Theta)},$$

$$\Phi_4 = \rho_c \int_{\Theta_2}^{\Theta_3} \frac{\rho_b(\Theta)\,\rho_{10}(\pi/2-\Theta)\exp(-2\varepsilon l/\cos\Theta)\,\mathrm{d}\Theta}{1-E\Theta\exp(-2\varepsilon l/\cos\Theta)},$$

$$E(\Theta) = \rho_{10}\rho_b(\Theta), \quad \delta\to 0, \quad \Theta_1 \leqslant \Theta_c = \arcsin\left(\frac{1}{n}\right),$$

$$\Theta_c > \arctan\left(\frac{g}{2}\right), \quad \Theta_2 = \arctan\frac{g-2\tan\Theta'}{4},$$

$\Theta_3 = \arctan(3g/2)$, ρ_{10} and ρ_{01} are the respective reflection coefficients from the SE – air and air – SE interfaces, ρ_c is the critical reflection coefficient, and $\rho_b(\Theta)$ is the substrate reflectance function at the light beam propagation angle Θ in the SE.

Each term in the sum Φ_i in Eqn (1) describes the contribution of different constituents of the flux, viz. Φ_1 is the contribution from multiple reflections of the beam incident normal to the element surface, Φ_2 is the contribution of the first reflection from the substrate in the angle interval $[\delta, \Theta_1]$ and of multiple reflections of the light flux from the butt-end surfaces of the SE, Φ_3 is the contribution of the first reflections from the substrate in the angle range $[\Theta_1, \Theta_2]$ that undergo CIR from the upper ES surface and form light fluxes whose high brightness is comparable to the first reflection, and Φ_4 is the contribution of reflections from the side surfaces of the SE.

Evaluation of the relative contributions of different flux constituents indicates that Φ_1 is smaller than Φ_2 and Φ_3. The magnitude of Φ_2 depends on the reflective properties of the substrate (the contribution of multiple reflections from the side surfaces being small). The contribution Φ_3 is comparable to Φ_2, and the upper boundary of the angle interval is determined by g. The contribution Φ_4 is smaller than Φ_1, Φ_2, and Φ_3 because the coefficients $\rho_b(\Theta)$ and $\rho_{10}(\pi/2-\Theta)$ are much smaller than 1; the angle interval $[\Theta_2, \Theta_3]$ being considered is also small and is close to $\pi/2$.

The largest contribution to I_Σ is made by the first reflection from the substrate and multiple (very bright) reflections depending on CIR conditions. For $g > 10$, the magnitude of I_Σ largely depends on the sums Φ_2 and Φ_3 making the greatest contribution to the resultant light field.

The dependence of the reflection coefficient $r(\Theta')$ on εl can be represented as

$$r(\Theta') = \frac{I_\Sigma}{I_{\Sigma 0}} = \frac{L}{L_0}\exp\left[-\varepsilon l\left(1+\frac{1}{\cos\Theta'}\right)\right], \tag{2}$$

where $I_{\Sigma 0}$ is the background signal (in the absence of photoabsorbing components) and Θ' is the light flux propagation angle outside the SE,

$$L = \sum_1^4 \Phi_i; \quad L_0 = \frac{E(0)}{1-E(0)} + \int_\delta^{\Theta_1} \frac{\mathrm{d}\Theta}{1-E(\Theta)} + \rho_c\left[\int_{\Theta_1}^{\Theta_2} \frac{\mathrm{d}\Theta}{1-E(\Theta)} + \int_{\Theta_2}^{\Theta_3} \frac{\rho_b(\Theta)\,\rho_{10}(\Theta')\,\mathrm{d}\Theta}{1-E(\Theta)}\right].$$

The calculations indicate (Fig. 4a) that even in the case of a poorly reflecting substrate ($\rho_{b0} = 0.1$) in the range $\varepsilon l \in (0; 0.1)$, absorption in the reflected light ($\ln r$) is much higher than in the transmitted light ($\ln t$) and depends on g. For example, the relative amplification of the informative signal $K = ln/ln$ at $el = 0.05$ must be $K = 2.5$ ($g = 2$), $K = 3.6$ ($g = 5$), and $K = 5.1$ ($g = 20$). At $\varepsilon l = 1.0$, $K = 2.4$ ($g = 2$) and $K = 3.1$ ($g = 20$).

The strength of the informative signal registered by a photoreceiver depends on the angle Θ' at which the reflected light flux is recorded and on the angle of the detector field of vision, which, similarly to g, must be chosen as required by the range and sensitivity of measurements.

Experimental verification of theoretical estimates (2) (Fig. 4b) was performed using sensor imitators in the form of HC6, HC7, HC8, HC9, and HC10 neutral glasses ($D = 6$ mm, $l = 0.3$ mm, $g = 20$) placed on a ftoroplast substrate. In the range $\varepsilon l \in (0; 0.1)$, we have $K = 5$, in agreement with the calculated values. In the range $\varepsilon l = 0.12-1.25$, the discrepancy between experimental findings and theoretical estimates did not exceed $\pm 5\%$. The reader is referred to Refs [23, 24] for a detailed discussion of theoretical and experimental data.

To conclude, it has been shown that measurements in reflected light lead to 'autoadjustment' of the optical path length. In other words, the smaller the concentration of the absorbing substance, the longer the optical path of the probing radiation, and vice versa (increased concentration is associated with a decrease in the optical path length). This finding provides a basis for the improvement of sensitivity of measurements at low concentrations and the extension of their dynamical range, i.e., for the creation of conditions allowing the use of a variety of methods to record the

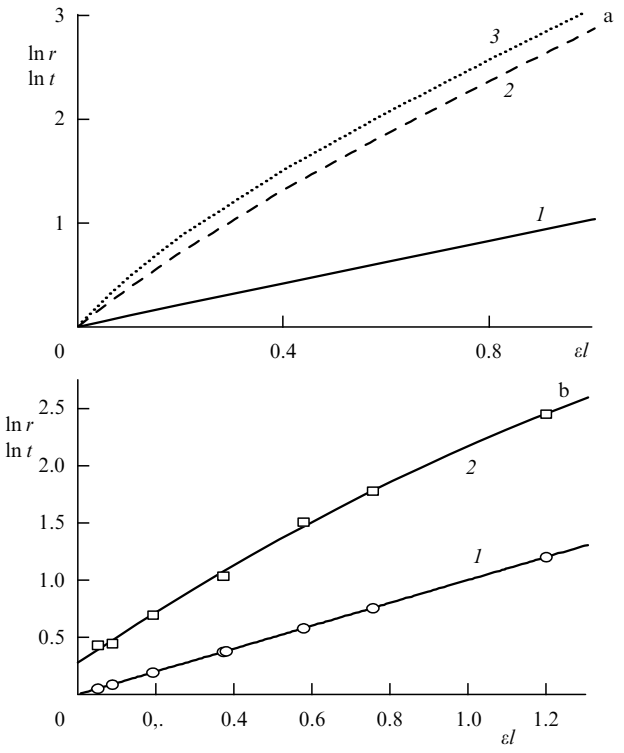

Figure 4. (a) Theoretical dependences of estimated logarithms of the transmission coefficient $\ln t$ (curve *1*) and reflection coefficient $\ln r$ on the value of εl for an SE ($n = 1.45$). Reflectance was estimated for the SE on a diffusely reflective substrate with $\rho_{b0} = 0.1$ at $g = 5$ (curve *2*) and $g = 20$ (curve *3*). (b) Experimental verification of the same dependences for a sensor simulator in transmitted (1) and reflected (2) light at $\lambda = 550$ nm and the reflected light angle 45°.

informative signal (not only by the end-point method but also using the kinetic approach [25, 26]). Kinetic measurements in transmitted light were carried out for the design of fast-acting sensors with the use of selective optically transparent plasticized membranes [25].

4. Study of properties and software–hardware realization of the recurrent algorithm for the evaluation of 'linear trend' signals

The available methods and tools allow analyzing samples using two signal recording modes, i.e., the end-point detection technique and the kinetic regime. In either case, the output signal of the detector has a determinate form with unknown informative parameters to be found. Conversion of the 'signal q–time t' coordinates by introducing a special time scale $\varphi(t)$ and transformation $x(q)$ gives the dependence in the form

$$x = a_0 + b_0\varphi(t) + \xi(t)\,, \tag{3}$$

where a_0 and b_0 are the sought informative parameters and $\xi(t)$ is the additive random noise with an a priori unknown distribution law.

The principal tasks include (a) analysis of the constituent signals of the 'linear trend' type (3); (b) the choice and investigation of algorithms for the evaluation of a_0 and b_0; (c) optimization of algorithms in accordance with the criteria for the minimization of errors and/or the use of computer resources; and (d) software–hardware realization. A series of our publications [27–29] were devoted to solving these problems.

In the majority of cases, the informative parameter is b_0. Passing to the first difference in the summation of trends (3) gives a totality of constant signals with an additive symmetric (hence, centered) noise. The latter problem is effectively resolved with the help of the Fabian–Tsypkin algorithm [30]:

$$c_{n+1} = c_n - \frac{\beta}{n}\,\Psi(c_n - x_{n+1})\,, \tag{4}$$

where

$$\Psi(z) = \begin{cases} -1, & z \leqslant -\Delta \\ 0, & |z| < \Delta \\ 1, & z \geqslant \Delta \end{cases},$$

$x_{n+1} = c^* + \xi_{n+1}$ is the measurement, ξ_{n+1} is the noise, c_n and c_{n+1} are values at the nth and $(n+1)$th estimation steps, β is the algorithm parameter, and 2Δ is the insensitivity zone size (in the case where $\Delta = 0$, $\Psi(z) = \mathrm{sign}(z)$). It is known [30, 31] that estimates ensuing from recurrent algorithm (4) are robust (resistant to bursts), unlike those obtained by the least-square method. The estimation efficiency is generally strongly dependent on the parameters (β, Δ) [31], whose choice is optimized by the criterion of a minimum of estimation error dispersion.

The formerly unexplored case of triangular-shaped (Simpson) noise as the first difference of uniformly distributed noises is described in [27]. It was demonstrated for the first time that only in this case, at the optimal β, Δ ratio, is the estimation error dispersion unrelated to the size of the insensitivity zone.

One of the basic results is the author's original interpretation of algorithm (4) as an automatic control system (ACS) [29] (Fig. 5), which allows the methods of ACSs to be used for the evaluation of its stability, that is, convergence between the estimated c_n and the true c^* values.

An ACS has the following main characteristics: (a) it is discrete, (b) it has two feedback contours, one of them being a negative feedback contour, (c) it contains a nonlinear element K_1 that realizes the function Ψ (a nonideal relay with the insensitivity zone 2Δ); (d) it contains a link with variable parameters $K_2[n]$ that realizes multiplication by β/n; and (e) it has a delay line with a one-step delay and the transfer characteristic K_3.

The conclusion obtained at in Ref. [29] that a given ACS is asymptotically stable in the presence of any zero insensitivity zone has been fully confirmed by other authors.

The following problems were resolved for the practical realization of algorithm (4) in the form of a computing device: (a) the choice of the parameters β and Δ based on extreme

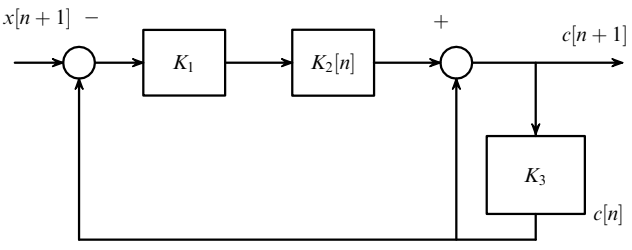

Figure 5. Schematic of an ACS realizing algorithm (3) (see text for the description).

order statistics requiring only a recurrent recalculation of the maximum and minimum elements; (b) the choice of the initial approximation of the estimate as the amplitude center (on the same basis); (c) substantiation of the criterion for the interruption of estimation (needed, for example, because of signal discordance, i.e., a change in the signal trend shape). In addition, we fixed the signs of the nonlinear term in Eqn (4) and constructed and assessed the asymmetry of their histogram [28, 29]. In other words, economical procedures were employed that required no ordering (the search for the median, bend center, etc.).

The device being considered realizes economical computation procedures by virtue of the effective estimation under conditions of the minimal a priori information about random noise parameters. This, in turn, allows realizing the possibility to develop and design a unified computation algorithm and a device compatible with a large variety of instruments for express analyses, including portable and subminiature ones.

5. Conclusion

The prediction and realization of new mechanisms underlying acceleration of immune reactions in HetIA opened up formerly unknown possibilities for the practical utilization of USSW fields

• to develop highly informative methods for the investigation of immunoactive phenomena at the molecular, supramolecular, and cellular levels and

• to construct highly selective devices for sample preparation.

We are currently developing instruments and methods to prepare samples for the identification and characterization of biological subjects based on the analysis of nucleic acid molecules (polymerase chain reaction, in particular, on a real-time scale). In these instruments, the isolation of biological subjects on immunosorbents placed in an USSW field prevents inhibition of the polymerase chain reaction by impurities. Express analysis of immunoactive phenomena containing no nucleic acids, e.g., toxins, is performed with the help of an immune reaction in the USSW field. The method is based on the results of fundamental research into the properties of US fields and the behavior of biological subjects in USSW fields (see Section 2).

The results of the theoretical analysis of the light flow distribution in a formerly unexplored subject of photometry, a thin optically transparent photoabsorbing element restricted in size, have allowed proposing a simple universal scheme of a detector (Fig. 6) that is easy to convert to a multichannel one, e.g., by using fiber-optic technologies [32]. This scheme has found application in a variety of instruments and devices constructed at the Institute of Analytical Instrumentation, Russian Academy of Sciences, that are now available commercially. These are the Imatest-01 analyzer of immunoactive subjects [33]; Nanofor-01 and Nanofor-02 analytical systems for high-performance capillary electrophoresis with spectrophotometric and fluorescent detectors; ANK-16, ANK-32, and ANK-96 nucleic acid analyzers; nucleic acid sequencer (ANPK); laser immunoluminescent cell analyzer; and the Sen and μSen chemosensor analyzers.

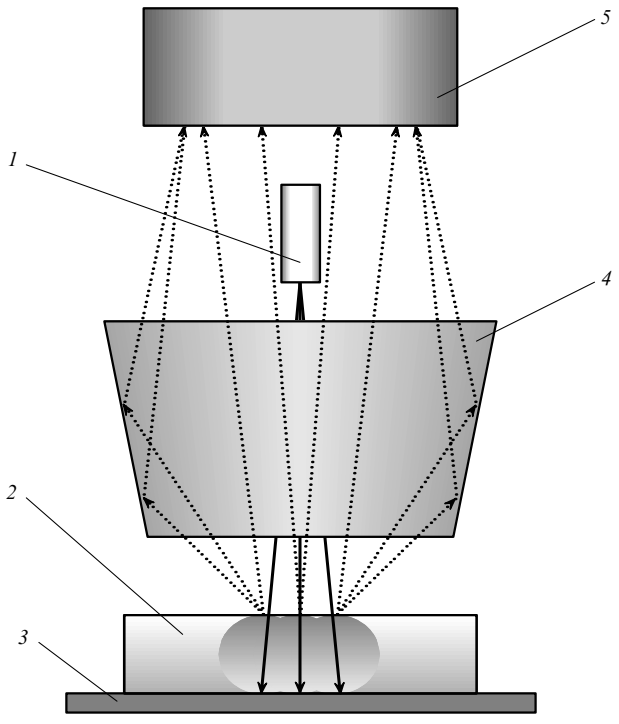

Figure 6. Optical scheme of a reflected light photometer: *1* — emission source, *2* — sensitive element (chemosensor), *3* — reflective substrate, *4* — radiation collector (elliptical mirror), *5* — photoreceiver.

References

1. Ngo T T, Lenhoff H M (Eds) *Enzyme-mediated Immunoassay* (New York: Plenum Press, 1985) [Translated into Russian (Moscow: Mir, 1988)]
2. Egorov A M et al. *Teoriya i Praktika Immunofermentnogo Analiza* (Theory and Practice of Enzyme-Mediated Immonoassay) (Moscow: Vysshaya Shkola, 1991)
3. Widder K J et al. *Clin. Immunol. Immunopathol.* **14** 395 (1979)
4. King L V *Proc. R. Soc. London Ser. A* **147** 212 (1934)
5. Yosioka K, Kawasima Y *Acustica* **5** (3) 167 (1955)
6. Gor'kov L P *Dokl. Akad. Nauk SSSR* **140** (1) 88 (1961) [*Sov. Phys. Dokl.* **6** 773 (1962)]
7. Knyaz'kov N N, Ph. D. Thesis of Technical Sciences (Pushchino: Institute of Biological Physics of the Academy of Sciences of USSR, 1983)
8. Zarembo L K, Krasil'nikov V A *Vvedenie v Nelineinuyu Akustiku* (Introduction to Non-Linear Acoustics) (Moscow: Nauka, 1966)
9. *Metodicheskie Rekomendatsii po Polucheniyu i Primeneniyu Immunoglobulinovogo Sefaroznogo Diagnostikuma dlya Indikatsii Vozbuditelya Ornitoza* (*Psittakoza*) *i Dvukh Vidov Khlamidiyi* (Guidelines on the Preparation and Application of Sepharose Iimmunoglobulin Diagnosticum for the Identification of the Pathogen of Ornithosis (Psittacosis) and Two Chlamydia Species) (Moscow: Minzdrav SSSR, 1981) p. 15
10. Blokhin K V et al. "Sposob postanovki serologicheskoi reaktsii" ("Method of realization of serological reaction"), USSR Inventor's Certificate 1208916, priority of 30.11.83 (1985)
11. Knyaz'kov N N, Kurochkin V E "Sposob vyyavleniya immunoaktivnykh ob'ektov" ("Method for the identification of immunoactive objects"), USSR Inventor's Certificate 1250576, priority of 13.01.84 (1986)
12. Knyaz'kov N N, Kurochkin V E *Byull. Eksp. Biol. Med.* (5) 586 (1996)
13. Spengler J F et al. *Bioseparation* **9** 329 (2000)
14. Morgan J et al. *Toxicology in Vitro* **18** 115 (2004)
15. Hawkes J J et al. *Biosensors Bioelectron.* **19** 1021 (2004)
16. Evstrapov A A, Kurochkin V E, Makarova E D *Nauchn. Priborostroenie* **1** (4) 22 (1991)
17. Gershun A A *Izbrannye Trudy po Fotometrii i Svetotekhnike* (Collected Works on Photometry and Phototechnique) (Moscow: GIFML, 1958)

18. Rozenberg G V *Usp. Fiz. Nauk* **69** (1) 57 (1959) [*Sov. Phys. Usp.* **2** 666 (1959)]
19. Rozenberg G V *Usp. Fiz. Nauk* **91** (4) 569 (1967) [*Sov. Phys. Usp.* **10** 188 (1967)]
20. Zege E P, Ivanov A P, Katsev O L *Perenos Izobrazheniya v Rasseivayushchei Srede* (Image Transfer in a Scattering Medium) (Minsk: Nauka i Tekhnika, 1985) [Translated into English: *Image Transfer Trough a Scattering Medium* (Berlin: Springer-Verlag, 1991)]
21. Ivanov A P *Optika Rasseivayushchikh Sred* (Optics of Scattering Media) (Minsk: Nauka i Tekhnika, 1969)
22. Loiko V A, in *Rasseyanie i Pogloshchenie Sveta v Prirodnykh i Iskusstvennykh Dispersnykh Sredakh* (Light Scattering and Absorption in Natural and Artificial Dispersed Media) (Ed. A P Ivanov) (Minsk: Inst. Fiziki im. B I Stepanova AN BSSR, 1991) p. 355
23. Evstrapov A A, Kurochkin V E *Opt. Zh.* **62** (2) 50 (1995)
24. Evstrapov A A, Kurochkin V E *Opt. Zh.* **62** (5) 40 (1995) [*J. Opt. Technol.* **62** 304 (1995)]
25. Kurochkin V E, Makarova E D *Analytical Commun.* **33** 115 (1996)
26. Burylov D A et al. *Zh. Analit. Khim.* **52** 551 (1997) [*J. Analytical Chem.* **52** 492 (1997)]
27. Bulyanitsa A L, Kurochkin V E *Avtomatika Telemekh.* (9) 187 (1999) [*Automat. Remote Control.* **60** 1368 (1999)]
28. Bulyanitsa A L, Kurochkin V E, Burylov D A *Radiotekh. Elektron.* **47** 343 (2002) [*J. Commun. Technol. Electron.* **47** 307 (2002)]
29. Bulyanitsa A L, Kurochkin V E *Nauchn. Priborostroenie* **12** (2) 30 (2002)
30. Tsypkin Ya Z, Polyak B T *Dinamika Sistem* (12) 22 (1977)
31. Bedel'baeva A A *Avtomatika Telemekh.* (1) 87 1978
32. Kurochkin V E, Evstrapov A A, Makarova E F "Opticheskoe ustroistvo dlya khimicheskogo analiza" ("Optical device for chemical analysis"), RF Patent 2157987, priority of 21.05.1996 (2000)
33. Fedorov A A et al. *Dokl. Ross. Akad. Nauk* **405** (1) 133 (2005) [*Dokl. Biochem. Biophys.* **405** 388 (2005)]

PACS numbers: 42.68.Wt, 95.55.Cs, 95.75.Qr

DOI: 10.1070/PU2006v049n09ABEH006106

Adaptive optical imaging in the atmosphere

V P Lukin

1. Introduction

As is well known, adaptive optics (AO) enjoys effective use in the formation of optical beams and images with the aim of concentrating laser beam energy, improving the sharpness of optical images, increasing the data transfer rate in optical communication lines, and solving other specific problems.

Investigations to develop methods and systems of adaptive optics are being pursued at the Laboratory of Coherent and Adaptive Optics of the Institute of Atmospheric Optics, Siberian Division of the Russian Academy of Sciences. This research is aimed at both elaborating the theory of adaptive systems and developing new elements, models of the systems, and their algorithms.

2. Problems in 'viewing' through the atmosphere

The bulk of information in astronomy is obtained by ground-based instruments. However, inhomogeneities of Earth's atmosphere (refraction, turbulence, radiation-absorbing gases, aerosols) seriously limit the capabilities of astronomical systems. In their papers in the late 1960s, Kolchinskii, Tatarski, and Frid formulated the atmosphere-imposed limitations on astronomical systems. Their results were obtained assuming the Kolmogorov–Obukhov model for the fluctuation spectrum of the refractive index:

$$\Phi_n(\varkappa, h) = 0.033 C_n^2(h)\,\varkappa^{-11/3}\,, \quad \frac{1}{L_0} \ll \varkappa \ll \frac{1}{l_0}\,.$$

Here, $C_n^2(h)$ is the structure parameter of the atmospheric refractive index, h is the current height above the underlying surface in the atmosphere, $\varkappa$ is the wavenumber for turbulent inhomogeneities, and L_0 and l_0 are the inner and outer turbulence scales.

Solving the problem of the optical wave propagation through randomly inhomogeneous media has shown that the phase structure function at a distance ρ obeys the five-thirds power law:

$$D_S(\rho) = 2.91\,k^2 \int_0^\infty \mathrm{d}h\, C_n^2(h)\,\rho^{5/3}\,,$$

where $k = 2\pi/\lambda$ and λ is the radiation wavelength. Proceeding from the last expression, the so-called atmosphere coherence radius r_0 was introduced:

$$D_S(\rho) = 2.91\,k^2 \int_0^\infty \mathrm{d}h\, C_n^2(h)\,\rho^{5/3} = 6.88\left(\frac{\rho}{r_0}\right)^{5/3}\,,$$

which determines the limiting angular resolution $\gamma_0 = \lambda/r_0$ of an optical system in the turbulent atmosphere, the Strehl parameter $\mathrm{St} = \exp(-\sigma^2)$ of the astronomical system atmosphere–telescope (where σ^2 is the variance of phase distortions), the optical transfer function, the point spread function, and other parameters of the astronomical instrument.

Research carried out in the 1960s showed that these theoretical results agree nicely with experimental data obtained for optical apertures of the order of 2–4 m. However, the effective apertures of ground-based astronomical telescopes began to increase swiftly: the 6 m BTA telescope (the Large Azimuth Telescope), the Multiple Mirror Telescope (MMT) with a matrix of six 8 m apertures, the 3.6 m New Technology Telescope (NTT), the 10 m Keck telescope, the 8.2 m Very Large Telescope Interferometer (VLTI), and the 8 m Subaru telescope made their appearance. In this connection, interest was aroused in the study of the phase fluctuations of optical waves in wide-aperture reception.

2.1 Phase fluctuations of optical waves in a turbulent atmosphere

The 1970s saw the development [1, 2] of interference wave phase meters in the optical range for the investigation of turbulent phase fluctuations of the optical wave for long spatial and temporal delays. The phase structure function was found to be sensitive both to the turbulence intensity and to the outer turbulence scale. This compelled reconsidering Tatarski's and Frid's results. In the early 1970s, measurements were made of optical wave phase fluctuations in the USSR (V Pokasov, V Lukin), Italy (L Ronchi, A Consortini), and the USA (G Ochs, S Clifford), with the result that the effect of 'phase structure function saturation' was discovered almost simultaneously [1, 2]. In Refs [1, 3, 4], this effect was interpreted and invoked to describe the spectrum of turbulence with a finite outer scale. We recall that the outer turbulence scale in the Kolmogorov–Obukhov model is assumed to be infinite.

In the 1970s and the 1980s, a consistent theory [1, 2] of phase fluctuations for optical waves propagating through a